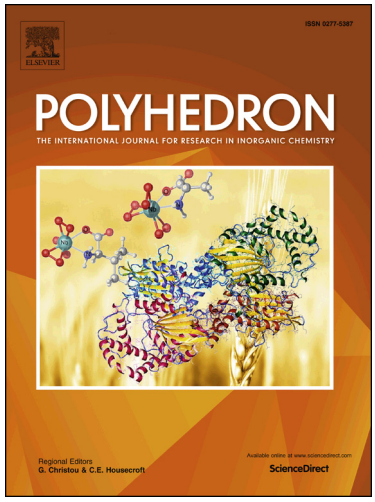


# Synthesis, characterization, theoretical and antimicrobial studies of tridentate hydrazone metal complexes of Zn(II), Cd(II), Cu(II) and Co(III)

Wei Cao, Yaoming Liu, Ting Zhang, Jinping Jia

PII: S0277-5387(18)30137-2
DOI: https://doi.org/10.1016/j.poly.2018.03.012
Reference: POLY 13078

To appear in: *Polyhedron*

Received Date: 29 January 2018
Accepted Date: 12 March 2018

Please cite this article as: W. Cao, Y. Liu, T. Zhang, J. Jia, Synthesis, characterization, theoretical and antimicrobial studies of tridentate hydrazone metal complexes of Zn(II), Cd(II), Cu(II) and Co(III), *Polyhedron* (2018), doi: https://doi.org/10.1016/j.poly.2018.03.012

# Synthesis, characterization, theoretical and antimicrobial studies of tridentate hydrazone metal complexes of Zn(II), Cd(II), Cu(II) and Co(III)

Wei Cao*, Yaoming Liu, Ting Zhang, Jinping Jia
*Scientific Instrument Center, Shanxi University, Taiyuan, 030006, P. R. China.*
E-mail: caowei@sxu.edu.cn

**Abstract**

The synthesis of four new complexes involving a tridentate hydrazone ligand ($H_2L$ = hydrazinyl-(pyridin-2-yl)salicyladimine) with Zn(II), Cd(II), Cu(II) and Co(III) ions is reported. Complexes $[Zn(HL)_2]$ (**1**), $[Cd(HL)_2]$ (**2**) and $[Cu_2(HL)_2(OAc)_2]$ (**3**) were synthesized by a one-pot reaction. A trivalent cobalt complex, $[Co(HL)_2]Cl(CH_3OH)$ (**4**), was obtained from the reaction of $H_2L$ with $CoCl_2$. The hydrazone ligand and the metal complexes were characterized by elemental analyses, IR and single-crystal X-ray diffraction. The location of the HOMO and LUMO frontier orbitals on the molecular structures of **1**-**4** were employed to explain influence of the central atoms on the electronic properties of the complexes. The antimicrobial activities of $H_2L$ and the metal complexes were investigated on three bacteria strains (*Staphylococcus aureus*, *Bacillus subtilis* and *Escherichia coli*).

***Keywords***: Schiff base complex; Hydrazone; Synthesis; Crystal structure; Antimicrobial activity

## 1. Introduction

Metal coordination compounds have been a subject of particular interest due to their broad range of applications in science and technology [1-3]. Among the various complexes, transition metal complexes containing a Schiff base ligand are important, mostly due to their important applications in various areas such as catalysis [4-6], chemosensors [7,8], luminescent materials [9,10], energy materials [11,12],

magneto-structural chemistry [13,14] and biological fields [15-19]. Schiff base complexes have been significantly active over the years because of the wide variety of possible structures for the ligands, depending on the aldehyde and amine used. Hydrazones, a member of the Schiff base family with a triatomic >C=N-NH- linkage, play an important role in the development of coordination chemistry. Reports on the synthesis, characterization and structural studies of hydrazone ligands show the importance of the hydrazone complexes in various fields, including analytical and biological fields [20-24]. Concerning the bioactivity, in many cases complexes display higher activity than the parent ligands [25-27], suggesting that preparation of new hydrazine complexes can be an interesting task to satisfy the requirements of an application.

With the above consideration in mind, we selected the Schiff base hydrazinyl-(pyridin-2-yl)salicyladimine ($H_2L$) as the target ligand. When a functional group (–OH) is present close to the azomethine group, the Schiff bases bear an excellent coordinating ability to act as multidentate ligands. We have synthesized four new metal compounds with different structures and have characterized these complexes by a series experiments. In addition, the antibacterial activities of $H_2L$ and the metal compounds were also studied.

## 2. Experimental

### *2.1 Materials and physical measurements*

Salicylaldehyde and 2-hydrazinopyridine were purchased from J&K Scientific and used without further purification. The other reagents and solvents were analytical grade reagents from Beijing Chemical Reagent Factory. Elemental analyses were conducted using a Vario EL elemental analyzer. Fourier transform infrared (FT-IR) spectra were measured on a Thermo Scientific Nicolet iS50 spectrometer. X-ray single crystal structures were determined on a Bruker D8 VENTURE diffractometer.

### *2.2. Synthesis of $H_2L$*

A methanol (2 mL) solution of salicylaldehyde (0.3 mmol, 0.030 mL) and

2-hydrazinopyridine (0.3 mmol, 0.033 g) was sealed in a Teflon-lined stainless steel autoclave and heated at 80 °C for 1 day, then cooled to room temperature. White crystals were obtained (yield 82.5%). Anal. Calcd for $C_{12}H_{11}N_3O$: C, 67.59; H, 5.20; N, 19.70. Found: C, 67.46; H, 5.57; N, 19.59%. IR ($cm^{-1}$): 2993m, 1600s, 1586s, 1496m, 1446s, 1309s, 1267m, 1156m, 770s, 751m.

*2.3. Synthesis of the metal complexes*

*2.3.1. Synthesis of [Zn(HL)$_2$]* (**1**)

A methanol (3 mL) solution of $Zn(OAc)_2{\cdot}2H_2O$ (0.1 mmol, 0.022 g), 2-hydrazinopyridine (0.2 mmol, 0.022 g) and salicylaldehyde (0.2 mmol, 0.020 mL) was sealed in a Teflon-lined stainless steel autoclave and heated at 80 °C for 3 days, then cooled to room temperature. Yellow crystals suitable for X-ray crystallography were obtained (yield 64.7%). Anal. Calcd for $C_{24}H_{20}N_6O_2Zn$: C, 58.84; H, 4.12; N, 17.16. Found: C, 58.61; H, 4.15; N, 16.95%. IR ($cm^{-1}$): 3040w, 3003w, 1622vs, 1597m, 1539s, 1481s, 1468s, 1443m, 1427m, 1333s, 1310m, 1287m, 1265w, 1198m, 1152m, 1099m, 1038m, 754m, 735m.

*2.3.2. Synthesis of [Cd(HL)$_2$]* (**2**)

The Cd(II) complex was synthesized similarly to the Zn(II) complex, except that $Zn(OAc)_2{\cdot}2H_2O$ was replaced by $Cd(NO_3)_2{\cdot}4H_2O$, to produce yellow needle-like crystals (yield 35.9%). Anal. Calcd for $C_{24}H_{20}CdN_6O_2$: C, 53.69; H, 3.75; N,15.65. Found: C, 53.52; H, 4.05; N, 15.56%. IR ($cm^{-1}$): 3166w, 1648vs, 1604s, 1486m, 1411m, 1303s, 1274vs, 1254s, 1212m, 1189s, 1098vs, 1039m, 999m, 860s, 756vs.

*2.3.3. Synthesis of [Cu$_2$(HL)$_2$(OAc)$_2$]* (**3**)

The Cu(II) complex was synthesized similarly to the Zn(II) complex, except that $Zn(OAc)_2{\cdot}2H_2O$ was replaced by $Cu(OAc)_2{\cdot}H_2O$, to produce black crystals (yield 2.3%). Anal. Calcd for $C_{28}H_{26}Cu_2N_6O_6$: C, 50.22; H, 3.91; N, 12.55. Found: C, 49.97; H, 3.76; N, 12.56%. IR ($cm^{-1}$): 3035w, 1710s, 1620vs, 1599s, 1485s, 1450m, 1400m, 1326s, 1308s, 1287m, 1265w, 1200m, 1099m, 1038m, 754m, 735m.

*2.3.4. Synthesis of [Co(HL)$_2$]Cl(CH$_3$OH)* (**4**)

A methanol (4 mL) solution of $CoCl_2 \cdot 2H_2O$ (0.1 mmol, 0.022 g) and $H_2L$ (0.2 mmol, 0.042 g) was sealed in a Teflon-lined stainless steel autoclave and heated at 80 °C for 6 hours, then cooled to room temperature. Dark red crystals suitable for X-ray crystallography were obtained (yield 60.6%). Anal. Calcd for $C_{25}H_{24}ClCoN_6O_3$: C, 54.51; H, 4.39; N, 15.26. Found: C, 54.58; H, 4.09; N, 15.29%. IR (cm$^{-1}$): 3040m, 1650vs, 1610m, 1484s, 1468s, 1431s, 1396m, 1305m, 1284m, 1269m, 1199m, 1155m, 1120m, 747m.

*2.4. X-ray crystallography*

Single-crystal X-ray diffraction data of $H_2L$, **1**, **2**, **3** and **4** were collected on a Bruker D8 VENTURE diffractometer with graphite monochromated Mo-Kα radiation (λ = 0.71073 Å) at 293 K. The structures were solved by the direct method [28] and refined by full matrix least squares based on $F^2$ using the SHELX 2014 program [29]. All non-hydrogen atoms were refined anisotropically. Hydrogen atoms were placed in calculated positions. The detailed crystallographic data and structure refinement parameters of the complexes are listed in Table 1 for comparison.

**Table 1**. Crystal data and structure refinement parameters of compounds $H_2L$, **1**, **2**, **3** and **4**.

| Compound | $H_2L$ | **1** | **2** | **3** | **4** |
|---|---|---|---|---|---|
| Formula | $C_{12}H_{11}N_3O$ | $C_{24}H_{20}N_6O_2Zn$ | $C_{24}H_{20}CdN_6O_2$ | $C_{28}H_{26}Cu_2N_6O_6$ | $C_{25}H_{24}ClCoN_6O_3$ |
| Fw | 213.24 | 489.83 | 536.86 | 669.62 | 550.88 |
| Crystal system, space group | Monoclinic, $P2_1/n$ | Orthorhombic, *Pbcn* | Orthorhombic, *Pbcn* | Monoclinic, $C2/c$ | Monoclinic, $P2_1/n$ |
| *a* (Å) | 4.66(7) | 20.66(2) | 20.77(4) | 24.85 (4) | 11.47 (6) |
| *b* (Å) | 21.10(3) | 9.11(7) | 8.99(2) | 8.30(1) | 18.86(1) |
| *c* (Å) | 10.90(2) | 11.28(9) | 11.49(2) | 15.19(3) | 11.55(6) |
| α (°) | 90 | 90 | 90 | 90 | 90 |

| | | | | | |
|---|---|---|---|---|---|
| β (°) | 94.2(2) | 90 | 90 | 120.7(6) | 98.9 (2) |
| γ (°) | 90 | 90 | 90 | 90 | 90 |
| *V* (Å$^3$) | 1069.6(3) | 2122.6(3) | 2145.4(7) | 2692.8(8) | 2468.4(2) |
| *Z*, calculated density (Mg/m$^3$) | 4, 1.324 | 4, 1.533 | 4, 1.662 | 4, 1.652 | 4, 1.482 |
| *F* (000) | 448 | 1008 | 1080 | 1368 | 1136 |
| Reflections collected/unique | 6325 / 2435 [R(int)=0.0252] | 13630 / 2443 [R(int)=0.0470] | 39095 / 2464 [R(int)=0.1044] | 20605 / 3085 [R(int)=0.0783] | 23620 / 6119 [R(int) = 0.0250] |
| Goodness-of-fit on F$^2$ | 1.022 | 1.062 | 1.024 | 1.106 | 1.035 |
| Final R indices [$I$>2σ($I$)] | $R_1$ = 0.0449, $wR_2$ = 0.1017 | $R_1$ = 0.0395, $wR_2$ = 0.0980 | $R_1$ = 0.0523, $wR_2$ = 0.1113 | $R_1$ = 0.0489, $wR_2$ = 0.1036 | $R_1$ = 0.0402, $wR_2$ = 0.1000 |
| *R* indices (all data) | $R_1$ = 0.0883, $wR_2$ = 0.1205 | $R_1$ = 0.0617, $wR_2$ = 0.1077 | $R_1$ = 0.0933, $wR_2$ = 0.1328 | $R_1$ = 0.0957, $wR_2$ = 0.1321 | $R_1$ = 0.0492, $wR_2$ = 0.1065 |

$R_1 = \Sigma(|F_o| - |F_c|)/|F_o|$; $wR_2 = \{\Sigma[(w|F^2_o| - |F^2_c|)^2/\Sigma w(F^2_o)^2]\}^{1/2}$.

*2.5. Calculation Methods*

In this work, density functional theory (DFT) calculations using the Gaussian 09 program were carried out at the B3LYP functional level [30]. Additionally, the basis set LANL2DZ was employed for the Zn, Cd, Cu and Co atoms, and the other atoms are described with 6-31+G(d) [31]. The CPCM [32,33] was also employed in the calculations, and the solvent was methanol. Complexes **1**, **2** and **3** are closed shell systems and for complex **4**, the spin state is two.

*2.6. Antimicrobial activity*

A microtitre bioassay was used to determine the antibacterial activity [34]. The compounds were dissolved in DMSO (20% of the final volume) and sterile water (80% of the final volume). The samples (200 μL) were two-fold serially diluted with culture medium in 96-well microplates to give concentrations from 0.001 to 0.660 mg/mL.

Amoxicillin was used as a positive control for each bacterium, with solvent and bacteria-free wells being included as negative controls. Microplates were covered and incubated at 37 °C for 24 h. To indicate bacterial growth, 40 µL of 0.2 mg/mL *p*-iodonitrotetrazoliumchloride (INT) were added to each well and incubated at 37 °C for 30 min. Clear wells with INT after incubation indicate inhibition of bacterial growth. The minimum inhibitory concentration (MIC) was considered to be the lowest concentration of the test substance exhibiting no visible growth of bacteria in the microplate well. The results were repeated in triplicate and are expressed in micromolar concentrations (µM).

## 3. Results and discussion

The hydrazone ligand $H_2L$ was prepared from the reaction of salicylaldehyde with 2-hydrazinopyridine as the literature reported [35,36]. The IR spectrum exhibit a *v* (C=N) vibration at 1600 $cm^{-1}$. The structure was confirmed by single-crystal X-ray crystallography (Fig.1). Both intramolecular and intermolecular hydrogen bonds could be observed in $H_2L$ (Fig. S1). Compounds **1**-**3** were obtained using two equivalents of salicylaldehyde and 2-hydrazinopyridine with one equivalent of the metal salts. Compound **4** was prepared from the direct reaction of $H_2L$ and $CoCl_2 \cdot 2H_2O$ in methanol. All the compounds are air and moisture stable crystals at room temperature.

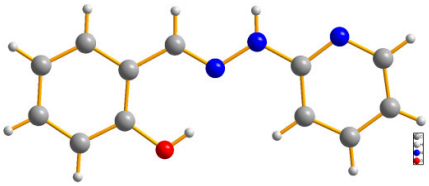

**Fig. 1**. Structure of $H_2L$.

*3.1. Description of the crystal structures*

*3.1.1. X-ray crystal structures of **1** and **2***

The *iso*-structural metal complexes **1** and **2** crystallize in the orthorhombic system with *Pbcn* space group, so only the Zn(II) complex (**1**) will be described. The analysis

of the $[Zn(HL)_2]$ coordination compound indicates that the ligand to metal ratio is 2:1. The molecular structure of **1** is shown in Fig. 2, and selected bond lengths and angles are summarized in Table 2. In the compound $[Zn(HL)_2]$, the Zn(II) atom is six coordinated by two Schiff base anion ligands. Each of the Schiff base ligands loses one hydrogen atom and coordinates to the metal ion through the hydrazine N atom and the phenolic O atom. The coordination environment can be best described as strongly distorted octahedral, as is often observed for hexacoordinated Zn(II) complexes. In this complex, the two deprotonated ligands are almost perpendicular to each other. The Zn(1)–O(1), Zn(1)–N(1) and Zn(1)–N(3) bond lengths are 2.073(2), 2.186(2) and 2.152(2) Å, respectively (Table 2), which are in agreement with the reported values for such bonds [37]. The crystal packing of complex **1** is stabilized mainly by N(2)–H(2A)···O(1) hydrogen bonds. As a result, a 1D polymeric chain is formed along the c-axis (Fig. 3, Table 3). Then, with the help of van der Waals (C(6)–H(6)···H(11)–C(11)) interactions, adjacent molecular units are linked together into an infinite 2-D supramolecular structure (Fig. S2). The structure of complex **2** is shown in the Supporting Information (Fig. S3-S5).

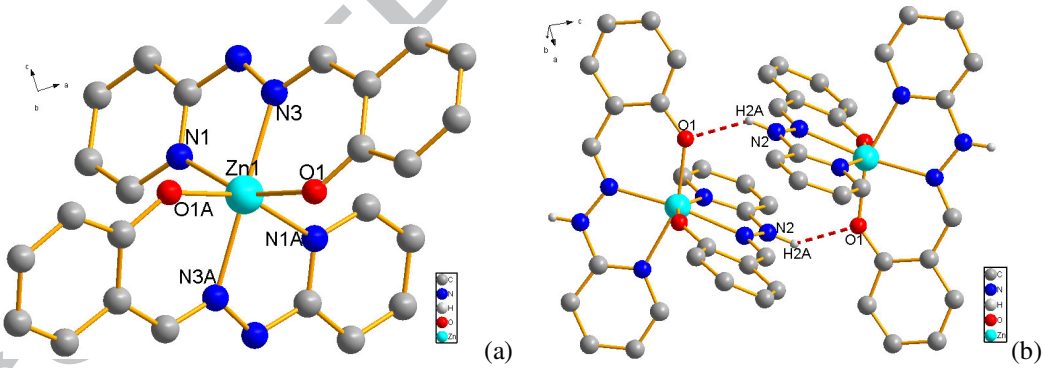


**Fig. 2**. (a) Crystal structure of complex **1**; (b) Intermolecular hydrogen bonds of **1**. The relevant coordination atoms are labelled. All H atoms are omitted for clarity, except those forming hydrogen bonds.

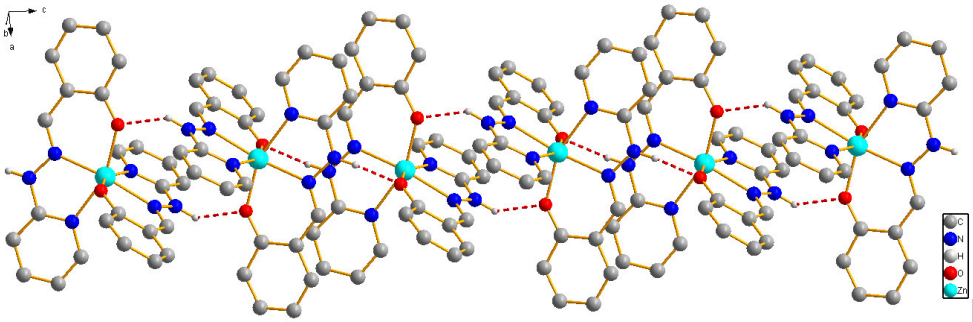


**Fig. 3**. The infinite 1-D chain supramolecular structure of **1**.

**Table 2**. Selected bond distances (Å) and angles (deg) for $H_2L$, **1**, **2**, **3** and **4**.

| | | | | | |
|---|---|---|---|---|---|
| | | | $H_2L$ | | |
| C(1)-N(1) | 1.343(2) | C(6)-N(3) | 1.282(2) | C(9)-C(10) | 1.371(3) |
| C(1)-C(2) | 1.368(2) | C(6)-C(7) | 1.448(2) | C(10)-C(11) | 1.376(3) |
| C(2)-C(3) | 1.367(2) | C(7)-C(12) | 1.396(2) | C(11)-C(12) | 1.376(2) |
| C(3)-C(4) | 1.371(2) | C(7)-C(8) | 1.401(2) | N(2)-N(3) | 1.359(2) |
| C(4)-C(5) | 1.391(2) | C(8)-O(1) | 1.357(2) | N(2)-H(2A) | 0.8600 |
| C(5)-N(1) | 1.333(2) | C(8)-C(9) | 1.382(2) | O(1)-H(1A) | 0.8200 |
| C(5)-N(2) | 1.377(2) | | | | |
| N(1)-C(1)-C(2) | 124.37(2) | C(12)-C(7)-C(8) | 117.57(2) | C(12)-C(11)-C(10) | 119.55(2) |
| C(3)-C(2)-C(1) | 118.02(2) | C(12)-C(7)-C(6) | 119.87(2) | C(11)-C(12)-C(7) | 121.64(2) |
| C(2)-C(3)-C(4) | 119.59(2) | C(8)-C(7)-C(6) | 122.56(1) | C(5)-N(1)-C(1) | 116.65(1) |
| C(3)-C(4)-C(5) | 118.67(2) | O(1)-C(8)-C(9) | 118.19(2) | N(3)-N(2)-C(5) | 119.70(1) |
| N(1)-C(5)-N(2) | 114.81(1) | O(1)-C(8)-C(7) | 121.39(1) | N(3)-N(2)-H(2A) | 120.1 |
| N(1)-C(5)-C(4) | 122.70(2) | C(9)-C(8)-C(7) | 120.42(2) | C(5)-N(2)-H(2A) | 120.1 |
| N(2)-C(5)-C(4) | 122.47(2) | C(10)-C(9)-C(8) | 120.48(2) | C(6)-N(3)-N(2) | 118.25(1) |
| N(3)-C(6)-C(7) | 122.00(1) | C(9)-C(10)-C(11) | 120.33(2) | C(8)-O(1)-H(1A) | 109.5 |
| | | | **1** | | |
| Zn(1)-N(1) | 2.186(2) | Zn(1)-O(1) | 2.073(2) | Zn(1)-N(3) | 2.152(2) |
| O(1)-Zn(1)-N(1) | 157.5(7) | O(1)-Zn(1)-N(1)$^a$ | 93.2(8) | N(3)-Zn(1)-N(1) | 74.1(7) |
| O(1)-Zn(1)-N(3) | 83.8(7) | O(1)$^a$-Zn(1)-O(1) | 89.3(1) | N(3)-Zn(1)-N(1)$^a$ | 95.9(7) |

| | | | | | |
|---|---|---|---|---|---|
| O(1)-Zn(1)-N(3)[a] | 106.5(7) | N(1)-Zn(1)-N(1)[a] | 92.9(1) | N(3)[a]-Zn(1)-N(3) | 165.8(1) |
| | | **2** | | | |
| Cd(1)-O(1) | 2.227(4) | Cd(1)-N(1) | 2.332(4) | Cd(1)-N(3) | 2.343(4) |
| O(1)-Cd(1)-N(1) | 148.5(1) | O(1)-Cd(1)-N(3) | 79.08(1) | N(1)-Cd(1)-N(3) | 69.71(1) |
| O(1)-Cd(1)-N(1)[b] | 94.8(2) | O(1)[b]-Cd(1)-O(1) | 92.1(2) | N(3)[b]-Cd(1)-N(3) | 166.5(2) |
| O(1)-Cd(1)-N(3)[b] | 110.6(1) | N(1)-Cd(1)-N(3)[b] | 100.8(1) | N(1)-Cd(1)-N(1)[b] | 95.2(2) |
| | | **3** | | | |
| Cu(1)-O(1) | 1.899(3) | Cu(1)-N(3) | 1.960(3) | Cu(1)-O(2) | 1.976(2) |
| Cu(1)-N(1) | 1.995(3) | Cu(1)-O(2)[c] | 2.393(2) | | |
| O(1)-Cu(1)-N(3) | 91.60(1) | N(3)-Cu(1)-O(2) | 171.75(1) | O(2)-Cu(1)-O(2)[c] | 78.07(9) |
| O(1)-Cu(1)-O(2) | 89.96(1) | N(3)-Cu(1)-N(1) | 80.45(1) | N(1)-Cu(1)-O(2)[c] | 95.33(1) |
| O(1)-Cu(1)-N(1) | 170.48(1) | N(3)-Cu(1)-O(2)[c] | 109.96(1) | O(2)-Cu(1)-N(1) | 97.19(1) |
| O(1)-Cu(1)-O(2)[c] | 92.29(1) | | | | |
| | | **4** | | | |
| Co(1)-O(2) | 1.880(1) | Co(1)-N(6) | 1.886(2) | Co(1)-N(3) | 1.888(2) |
| Co(1)-O(1) | 1.891(1) | Co(1)-N(1) | 1.934(2) | Co(1)-N(4) | 1.943(2) |
| O(2)-Co(1)-N(6) | 94.79(6) | N(6)-Co(1)-N(3) | 176.67(7) | N(3)-Co(1)-O(1) | 94.72(7) |
| O(2)-Co(1)-N(3) | 87.19(7) | N(6)-Co(1)-N(1) | 94.43(7) | N(3)-Co(1)-N(1) | 82.96(7) |
| O(2)-Co(1)-O(1) | 90.44(7) | N(6)-Co(1)-O(1) | 87.95(6) | N(3)-Co(1)-N(4) | 94.83(7) |
| O(2)-Co(1)-N(4) | 177.96(7) | N(6)-Co(1)-N(4) | 83.18(7) | O(1)-Co(1)-N(1) | 177.06(7) |
| O(2)-Co(1)-N(1) | 87.65(7) | N(1)-Co(1)-N(4) | 92.36(7) | O(1)-Co(1)-N(4) | 89.64(7) |

[a] Symmetry code: (-*x*+1, *y*, -*z*+1/2). [b] Symmetry code: (-*x*+1, *y*, -*z*+3/2). [c] Symmetry code: (-*x*+1, -*y*+1, -*z*+1).

### *3.1.2. X-ray crystal structure of **3***

Compound **3** crystallizes in the monoclinic space group *C*2/*c* and features a dimeric Cu(II) moiety. X-ray crystal structure analysis reveals that **3** forms a 2:2 ligand to metal stoichiometry and consists of two Cu(II) ions, two deprotonated ligands (HL) and two acetate anions. Fig. 4a shows the molecular structure of **3** and the

coordination configuration. The geometries of the Cu(II) atoms can be best described as slightly distorted square-pyramidal, with a $CuN_2O_3$ coordination. In this complex the O(1), N(1), O(2) and N(3) donors define the equatorial plane, with the Cu(II) atom lying in this plane, and the O(2A) (Symmetry code: -*x*+1, -*y*+1, -*z*+1) donor occupies the apical position. Bond lengths in the coordination sphere follow a wide range (Cu(1)–O(1) = 1.899(3) Å, Cu(1)–N(1) = 1.995(3) Å, Cu(1)–O(2) = 1.976(2) Å, Cu(1)–O(2A) = 2.393(2) Å, Cu(1)–N(3) = 1.960(3) Å). The oxygen atoms O(2) and O(2A) from two acetate ions linked the two Cu(II) atoms at distances of 1.976(2) and 2.393(2) Å. All the coordination distances are in the normal ranges, consistent with those for comparable copper(II) coordination environments [38,39]. In a previous study, $H_2L$ has been used with copper chloride to generate a 1 D coordination polymer. The introduction of a methoxy substituent on the phenol ring of $H_2L$ converts the original 1 D polymeric complex into a dinuclear complex [36]. In compound **3**, as shown in Figs. 5 and S6, intermolecular hydrogen bonds, N(2)-H(2)···O(3) and C(4)-H(4)···O(3) with distances of 2.745 and 3.487 Å respectively, produce a supramolecular polymeric association within 2D sheets.

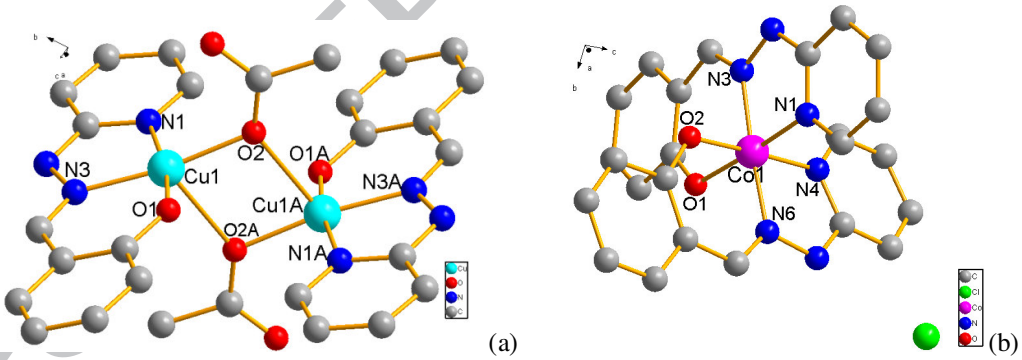


**Fig. 4**. (a) Crystal structure of complex **3**; (b) Crystal structure of complex **4**. The relevant coordination atoms are labelled. All H atoms are omitted for clarity.

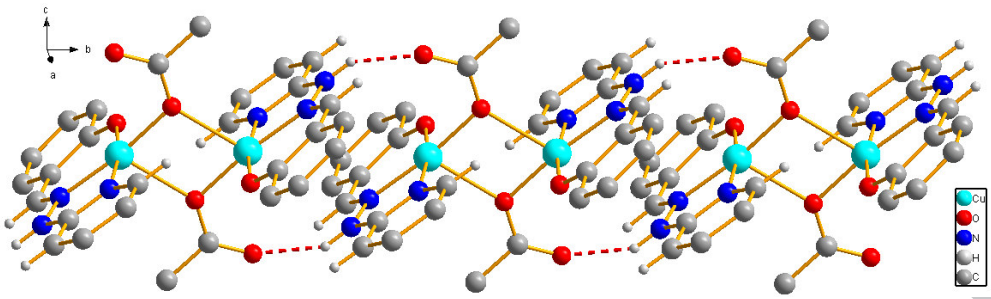


**Fig. 5**. 1-D chain supramolecular structure of **3** formed via hydrogen bonds (dark red)**.**

*3.1.3. X-ray crystal structure of **4***

Complex **4** has been prepared via the reaction of $H_2L$ with $CoCl_2{\cdot}2H_2O$ in methanol, however, over the course of the coordination reaction the divalent cobalt ion is oxidized to the Co(III) ion. In the structure, the cobalt centre features the anticipated six-coordinate geometry with bond distances typical for trivalent cobalt (all distances less than 2 Å) and similar to related Co(III) complexes previously reported [40,41]. The geometry of the coordination sphere is best considered to be octahedral (Fig. 4b). In this complex the O(1), N(1), N(3) and N(6) donors define the equatorial plane and the Co(III) atom lies in this plane. The O(2) and N(4) donors occupy the apical positions with an O-Co-N angle of 177.96(7)°. The $CoN_4O_2$ sphere thus formed is like the $FeN_4O_2$ sphere observed for Fe(III) complexes by Kou and co-workers [42]. An uncoordinated $Cl^-$ anion is present, thereby balancing the charge of the complex. In the structure of **4**, the non-bonded nitrogen atoms at the center of the ligand are protonated and form intramolecular hydrogen bonds to adjacent chloride atoms, which assist in the formation of a 1D chain (Fig. 6). In addition, one co-crystallized solvent methanol molecule was also found in the X-ray structure (Fig. S7).

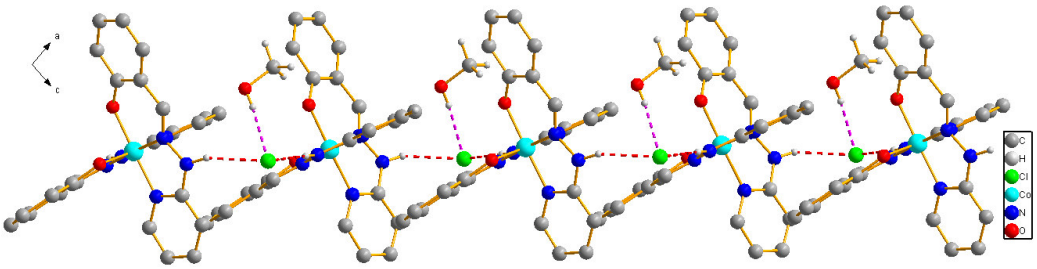


**Fig. 6.** 1-D chain supramolecular structure of **4** combined via hydrogen bonds (dark red)**.**

**Table 3**. Hydrogen bonding distances (Å) and angles (°) for complexes **1**, **2**, **3** and **4**.

| | D-H···A | d(D-H) | d(H···A) | d(D···A) | ∠DHA | Symmetry code |
|---|---|---|---|---|---|---|
| **1** | N(2)-H(2A)···O(1) | 0.860 | 2.068 | 2.745 | 135.06 | x, -y, z-1/2 |
| **2** | N(2)-H(13)···O(1) | 0.903 | 1.912 | 2.751 | 153.68 | x, -y+1, z-1/2 |
| **3** | N(2)-H(2)···O(3) | 0.860 | 1.978 | 2.745 | 147.87 | -x+1, -y, -z+1 |
| | C(1)-H(1)···O(1) | 0.930 | 2.560 | 3.209 | 127.21 | -x+1, -y+1, -z+1 |
| | C(4)-H(4)···O(3) | 0.930 | 2.577 | 3.487 | 166.16 | x, -y, z-1/2 |
| | C(6)-H(6)···O(3) | 0.930 | 2.572 | 3.270 | 132.17 | -x+1, -y, -z+1 |
| **4** | O(3)-H(3A)···Cl(1) | 0.820 | 2.294 | 3.111 | 174.34 | |
| | N(2)-H(26)···Cl(1) | 0.818 | 2.340 | 3.156 | 175.31 | |
| | N(5)-H(27)···Cl(1) | 0.889 | 2.374 | 3.192 | 152.87 | x+1/2, -y+1/2, z+1/2 |
| | C(1)-H(1)··· N(6) | 0.930 | 2.564 | 3.033 | 111.66 | |
| | C(1)-H(1)···O(3) | 0.930 | 2.514 | 3.374 | 154.02 | x+1/2, -y+1/2, z+1/2 |
| | C(2)-H(2)···O(2) | 0.930 | 2.615 | 3.458 | 151.06 | x+1/2, -y+1/2, z+1/2 |
| | C(13)-H(13)··· N(3) | 0.930 | 2.632 | 3.084 | 110.54 | |

*3.2. Theoretical studies*

To better understand the influence of the Zn(II), Cd(II), Cu(II) and Co(III) ions on the electronic properties of $H_2L$, density functional theory (DFT) calculations using the Gaussian 09 program were carried out at the B3LYP/6-31+G(d) level [30]. Selected optimized bond distances of these complexes are given in Table S1. From Table S1, it can be seen that the calculated bond lengths are in good agreement with the experimental measurements. Therefore, the theoretical method and basis set that we employed are suitable for geometry optimizations of the studied systems. The optimized structures, distributions on the highest occupied molecular orbitals (HOMOs) and lowest unoccupied molecular orbitals (LUMOs) of complexes **1**-**4** are shown in Fig. 7. The HOMOs and the LUMOs of **1** and **2** are promotions of electrons delocalized predominantly all over the molecules. The HOMO of **3** is similar to that of **1**, but the LUMO was mostly positioned at the center of the molecule. For

compound **4**, the $\alpha$-HOMO, $\beta$-HOMO and $\alpha$-LUMO were delocalized throughout the entire molecule, while the $\beta$-LUMO was mostly positioned at the center of the molecule. The computed energy levels of the HOMOs and LUMOs for **1**-**4** are shown in Table 4; it can be seen from Table 4 that a change of the central atom has a great influence on the frontier molecular orbital energy level. Therefore, the central atoms have an obvious influence on the electron distributions of the frontline molecular orbitals.

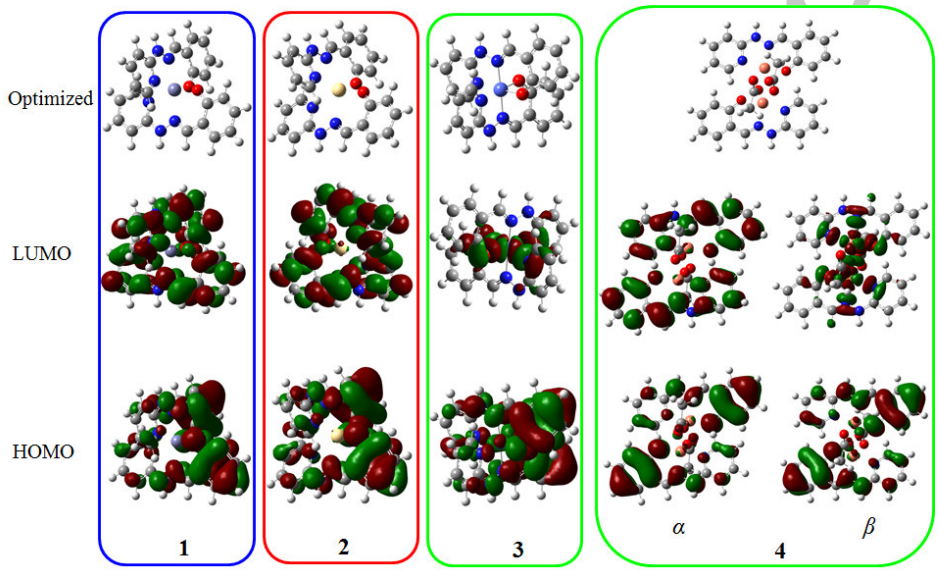


**Fig. 7**. HOMO and LUMO graphical representation of each molecule of the compounds.

**Table 4**. Computed energy levels (eV) of the HOMOs and LUMOs for complexes **1**, **2**, **3** and **4**.

| | **1** | **2** | **3** | **4** | |
|---|---|---|---|---|---|
| | | | | $\alpha$ | $\beta$ |
| HOMO | -5.01 | -4.98 | -5.74 | -5.45 | -5.40 |
| LUMO | -1.43 | -1.35 | -2.42 | -1.72 | -2.85 |
| $\Delta E_{H-L}$ | 3.58 | 3.63 | 3.32 | 3.73 | 2.55 |

*3.3. Antimicrobial activity*

The antibacterial activities of the hydrazone ligand $H_2L$ as well as its metal

complexes were tested against *Staphylococcus aureus* and *Bacillus subtilis* as Gram-positive and *Escherichia coli* as a Gram-negative microorganisms. The obtained results were compared with amoxicillin as a standard, with different concentrations.

As shown in Table 5, the hydrazone ligand and its metal complexes had different behavior against the same bacteria. $H_2L$ was significantly more toxic against Gram-positive than Gram-negative bacteria, which may be due to the different cell wall structures of the tested microorganisms [43]. Complexes **2**-**4** were found to have higher activity than **1** against the bacteria strains studied under the test conditions. In the *Bacillus subtilis* strains, $H_2L$ showed an outstanding activity among all the compounds tested, exhibiting a MIC value of 0.6 μM, even better than the effect of amoxicillin. For the *Staphylococcus aureus* strains, although amoxicillin was the most effective compound, **2** and **3** showed excellent activities, with MIC values of 5 and 7 μM. In addition, with the *Escherichia coli* strains, **3** and **4** showed outstanding activity, both with MIC values of 40 μM.

The results obtained revealed that the active complexes show, in general, higher antimicrobial properties than the ligand. Complex **3** was the most active among the series of diverse metal complexes. According to chelating theory, chelation could enhance the lipophilicity of the molecules, favoring permeation of the complexes through the lipid layer of the cell membrane [44,45]. Besides the chelate effect, the following factors should also be considered: (i) the nature of the metal centre, *i.e.* copper is an element with antimicrobial properties; (ii) the nuclearity of the metals in a complex, with dinuclear complexes usually being more potent than mononuclear ones [46,47]. In addition, variation of the antimicrobial activities of metal complexes against different bacteria depends on the impermeability of the cell or differences in the ribosomes in the microbial cells [48].

**Table 5**. Minimal inhibitory concentrations (MICs) of $H_2L$, **1**, **2**, **3** and **4** against bacterial strains.

| Compound | MIC (μM) |
|---|---|

| | *Escherichia coli* | *Staphylococcus aureus* | *Bacillus subtilis* |
|---|---|---|---|
| $H_2L$ | 400 | 60 | 0.6 |
| **1** | 600 | 700 | 700 |
| **2** | 200 | 5 | 8 |
| **3** | 40 | 7 | 4 |
| **4** | 40 | 400 | 60 |
| Amoxycilin | 200 | 0.04 | 12 |

## Conclusions

In this work, the tridentate Schiff base ligand $H_2L$, containing -NH-N=CH- and -OH groups, was synthesized. Zinc(II), cadmium(II), copper(II) and cobalt(III) complexes with this ligand were prepared by two methods and characterized by single-crystal X-ray diffraction. The mononuclear complexes $[M(HL)_2]$ (M(II) = Zn, Cd) and dinuclear copper(II) complex $[Cu_2(HL)_2(OAc)_2]$ were synthesized by a one pot reaction of salicylaldehyde, 2-hydrazinopyridine and the corresponding metal salts. The Co(III) Schiff-base complex ($[Co(HL)_2]Cl(CH_3OH)$) has been prepared in $CH_3OH$ via the reaction of $H_2L$ with $CoCl_2$, in which the Co(II) core was oxidized to Co(III). Hydrogen bonds play a crucial role in the construction of 1-D chains and 2-D layers in all the supramolecular metal complexes. The location of the HOMO and LUMO graphics help us to better understand the electronic properties of the complexes. $H_2L$ and the three metal complexes have antibacterial activities. However, the metal complexes have more excellent antibacterial properties, which are possibly attributed to the nature of metal center and the structure of the metal complexes. These observations have been guiding us for the development of new hydrazide derivatives and their metal complexes that possess varied biological activities.

.

## Acknowledgements

We are thankful for financial support from the Fundamental Research Funds for Shanxi University (No. 304545009) and the Natural Science Foundation of Shanxi

Province in China (No. 201701D221031). The theoretical studies were supported by the high- performance computing platform of Shanxi University

**Appendix A. Supplementary data**

CCDC 1826685, 1583570, 1583571, 1583572 and 1583573 contain the supplementary crystallographic data for complexes $H_2L$, **1**, **2**, **3** and **4**. These data can be obtained free of charge via http://www.ccdc.cam.ac.uk/conts/retrieving.html, or from the Cambridge Crystallographic Data Centre, 12 Union Road, Cambridge CB2 1EZ, UK; fax: (+44) 1223-336-033; or e-mail: deposit@ccdc.cam.ac.uk.

**References**

[1] W. Zhang, H.-Y. Ye, H.-L. Cai, J.-Z. Ge, R.-G. Xiong, S.D. Huang, J. Am. Chem. Soc. 132 (2010) 7300.

[2] S. Shibata, K. Tsuge, Y. Sasaki, S. Ishizaka, N. Kitamura, Inorg. Chem. 54 (2015) 9733.

[3] J.-N. Rebilly, B. Colasson, O. Bistri, D. Over, O. Reinaud, Chem. Soc. Rev. 44 (2015) 467.

[4] M.-F. Zaltariov, V. Vieru, M. Zalibera, M. Cazacu, N.M.R. Martins, L.M.D.R.S. Martins, P. Rapta, G. Novitchi, S. Shova, A.J.L. Pombeiro, V.B. Arion, Eur. J. Inorg. Chem. 37 (2017) 4324.

[5] P.G. Cozzi, Chem. Soc. Rev. 33 (2004) 410.

[6] T. Maity, D. Saha, S. Bhunia, P. Brandão, S. Das, S. Koner, RSC Adv. 5 (2015) 82179.

[7] W. Cao, X.-J. Zheng, D.-C. Fang, L.-P. Jin, Dalton Trans. 43 (2014) 7298.

[8] M. Parsaei, Z. Asadi, S. Khodadoust, Sens. Actuators, B 220 (2015) 1131.

[9] S. Wang, X. Yang, T. Zhu, L. Bo, R. Wang, S. Huang, C. Wang, D. Jiang, H. Chen, R.A. Jones, Dalton Trans. 47 (2018) 53.

[10] Y. Wang, P.-D. Mao, W.-N. Wu, X.-J. Mao, Y.-C. Fan, X.-L. Zhao, Z.-Q. Xu, Z.-H. Xu, Sens. Actuators, B 255 (2018) 3085.

[11] A. Kumar, D. Lionetti, V.W. Day, J.D. Blakemore, Chem. Eur. J. 24 (2018) 141.

[12] J. Zhang, L. Xu, W.-Y. Wong, Coord. Chem. Rev. 355 (2018) 180.

[13] W.K. Dong, J.C. Ma, L.C. Zhu, Y. Zhang, New J. Chem. 40 (2016) 6998.

[14] M. Fondo, J. Corredoira-Vázquez, A. Herrera-Lanzós, A.M. García-Deibe, J. Sanmartín-Matalobos, J.M. Herrera, E. Colacio, C. Nuñez, Dalton Trans. 46 (2017) 17000.

[15] M. Gaber, H.A. El-Ghamry, S.K. Fathalla, M.A. Mansour, Mat. Sci. Eng. C-Mater 83 (2018) 78.

[16] L.-Q. Chai, K.-Y. Zhang, L.-J. Tang, J.-Y. Zhang, H.-S. Zhang, Polyhedron 130 (2017) 100.

[17] R. Bonsignore, F. Russo, A. Terenzi, A. Spinello, A. Lauria, G. Gennaro, A.M. Almerico, B.K. Keppler, G. Barone, J. Inorg. Biochem. 178 (2018) 106.

[18] W.-J. Lian, X.-T. Wang, C.-Z. Xie, H. Tian, X.-Q. Song, H.-T. Pan, X. Qiao, J.-Y. Xu, Dalton Trans. 45 (2016) 9073.

[19] V.K. Singh, R. Kadu, H. Roy, P. Raghavaiah, S.M. Mobin, Dalton Trans. 45 (2016) 1443.

[20] F.-U. Rahman, M.Z. Bhatti, A. Ali, H.-Q. Duong, Y. Zhang, B. Yang, S. Koppireddi, Y. Lin, H. Wang, Z.-T. Li, D.-W. Zhang, Eur. J. Med. Chem. 143 (2018) 1039.

[21] M. Sutradhar, Rajeshwari, T.R. Barman, A. R. Fernandes, F. Paradinha, C. Roma-Rodrigues, M.F.C.Guedes da Silva, A.J.L. Pombeiro, J. Inorg. Biochem. 175 (2017) 267.

[22] R. Narang, B. Narasimhan, S. Sharma, Curr. Med. Chem. 19 (2012) 569.

[23] R. Fekri, M. Salehi, A. Asadi, M. Kubicki, Polyhedron 128 (2017) 175.

[24] D.A. Megger, K. Rosowski, C. Radunsky, J. Kösters, B. Sitek, J. Müller, Dalton Trans. 46 (2017) 4759.

[25] N. Farrel, Coord. Chem. Rev. 232 (2002) 1.

[26] M.-X. Li, D. Zhang, L.-Z. Zhang, J.-Y. Niu, B.-S. Ji, J. Organomet. Chem. 696 (2011) 852.

[27] C. González-García, A. Mata, F. Zani, M.A. Mendiola, E. López-Torres, J. Inorg. Biochem. 163 (2016) 118.

[28] G.M. Sheldrick, Acta Crystallogr. Sect. A 71 (2015) 3.

[29] G.M. Sheldrick, Acta Crystallogr. Sect. C 71 (2015) 3.

[30] M.J. Frisch, G.W. Trucks, H.B. Schlegel, G.E. Scuseria, M.A. Robb, J.R. Cheeseman, G. Scalmani, V. Barone, B. Mennucci, G.A. Petersson, H. Nakatsuji, M. Caricato, X. Li, H.P. Hratchian, A.F. Izmaylov, J. Bloino, G. Zheng, J.L. Sonnenberg, M. Hada, M. Ehara, K. Toyota, R. Fukuda, J. Hasegawa, M. Ishida, T. Nakajima, Y. Honda, O. Kitao, H. Nakai, T. Vreven, J.A. Montgomery, Jr., J.E. Peralta, F. Ogliaro, M. Bearpark, J.J. Heyd, E. Brothers, K.N. Kudin, V.N. Staroverov, R. Kobayashi, J. Normand, K. Raghavachari, A. Rendell, J.C. Burant, S.S. Iyengar, J. Tomasi, M. Cossi, N. Rega, J.M. Millam, M. Klene, J.E. Knox, J.B. Cross, V. Bakken, C. Adamo, J. Jaramillo, R. Gomperts, R.E. Stratmann, O. Yazyev, A.J. Austin, R. Cammi, C. Pomelli, J.W. Ochterski, R.L. Martin, K. Morokuma, V.G. Zakrzewski, G.A. Voth, P. Salvador, J.J. Dannenberg, S. Dapprich, A.D. Daniels, O. Farkas, J.B. Foresman, J.V. Ortiz, J. Cioslowski, D.J. Fox, Gaussian 09W, revision A.02; Gaussian, Inc.: Wallingford, CT, 2009.

[31] A.D. Becke, J. Chem. Phys. 65 (1982) 239.

[32] M. Cossi, V. Barone, R. Cammi, J. Tomasi, Chem. Phys. Lett. 255 (1996) 327.

[33] G. Scalmani, M.J. Frisch, J. Chem. Phys. 132 (2010) 114110.

[34] J.L. Rios, M.C. Recio, A. Villar, J. Ethnopharma. 23 (1988) 127.

[35] A. Sarkar, S. Pal, Polyhedron 25 (2006) 1689.

[36] J. Tang, J.S. Costa, A. Pevec, B. Kozlevcar, C. Massera, O. Roubeau, I. Mutikainen, U. Turpeinen, P. Gamez, J. Reedijk, Cryst. Growth Des. 8 (2008) 1005.

[37] B. Naskar, R. Modak, D.K. Maiti, M.G.B. Drew, A. Bauzá, A. Frontera, C.D. Mukhopadhyay, S. Mishra, K.D. Sahae, S. Goswami, Dalton Trans. 46 (2017) 9498.

[38] P. Gluzinski, J.W. Krajewski, Z. Urbanczyklipkowska, G.D. Andreetti, G. Bocelli, Acta Crystallogr. C 40 (1984) 778.

[39] S. Mukherjee, C. Basu, S. Chowdhury, A.P. Chattopadhyay, A. Ghorai, U. Ghosh, H. Stoeckli-Evans, Inorg. Chim. Acta 363 (2010) 2752.

[40] N.V. Dammea, V. Zaliskyy, A.J. Lough, M.T. Lemaire, Polyhedron 89 (2015)155.

[41] R.A. Taylor, N.M. Bonanno, D. Mirza, A.J. Lough, M.T. Lemaire, Polyhedron 131 (2017) 34.

[42] J. Yuan, M.-J. Liu, C.-M. Liu, H.-Z. Kou, Dalton Trans. 46 (2017) 16562.

[43] J.R. Anacona, J.L. Rodriguez, J. Camus, Spectrochim. Acta A 129 (2014) 96.

[44] S.J. Lippard, J.M. Berg, Principles of Bioorganic Chemistry, University Science Book, Mill Valley, 1994.

[45] G. Yang, J.Z. Wu, L. Wang, L.N. Ji, X. Tian, J. Inorg. Biochem. 66 (1997) 141.

[46] A.D. Russell, in Disinfection, Sterilization and Preservation, Lippincott Williams & Wilkins, Philadelphia, 2001.

[47] G. Psomas, D.P. Kessissoglou, Dalton Trans. 42 (2013) 6252.

[48] P.G. Lawrence, P.L. Harold, O.G. Francis, Antibiot. Chemother. 4 (1957) 1980.

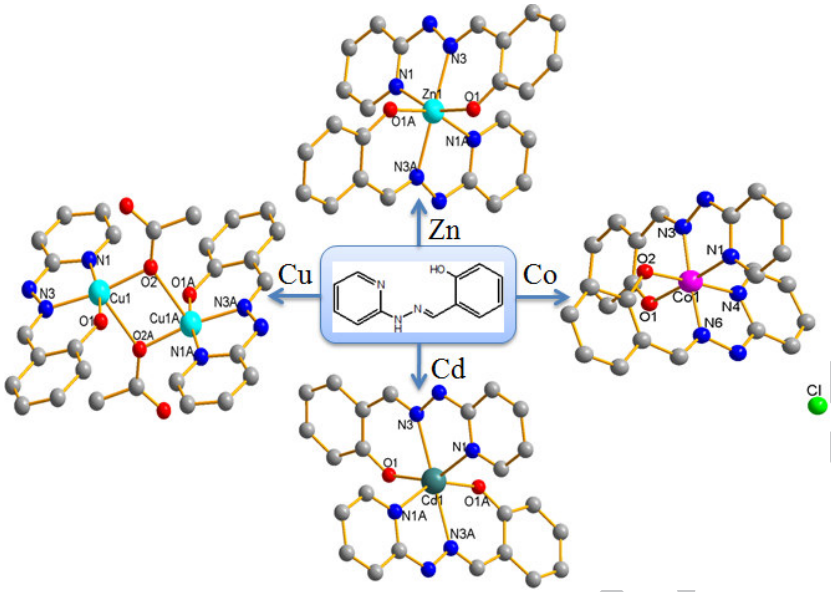

A series of complexes encompassing hydrazinyl-(pyridin-2-yl)salicyladimine as a ligand have been synthesized and structurally characterized. X-ray studies revealed that these complexes display mononuclear or binuclear structures with different coordination geometries. Antibacterial assays were carried out and DFT calculations were used to explain the influence of the metal ions on the electronic properties of the complexes.